2021 7th International Conference on Mechanical Engineering and Automation Science (ICMEAS) | 978-1-7281-9768-5/21/$31.00 ©2021 IEEE | DOI: 10.1109/ICMEAS54189.2021.00017

# Attitude Control of the Low Earth Orbit Satellite with Moving Masses under Strong Aerodynamic Disturbance

Yuandong Hu, Zhengliang Lu, Wenhe Liao, Xiang Zhang
Nanjing University of Science and Technology
School of Mechanical Engineering
Nanjing, China
e-mail: huyuandong@njust.edu.cn

***Abstract*—This study investigates an attitude control scheme for the satellite with moving masses and reaction wheels to solve the problem of the strong aerodynamic disturbance in low Earth orbit. The moving mass actuator is introduced to minimize the influence of the aerodynamic torque, so as to avoid the frequent saturation of the reaction wheel speed. The rotational dynamic equations of the attitude and the translational dynamic equations of the masses are derived by Newtonian mechanics. The dynamic effects of the mass movement are analyzed. A nonlinear observer is used for the precise estimation of the system disturbance to minimize the effects of the disturbance on attitude control through feedforward compensation. An incremental discrete PID control algorithm is used to slow down the mass movement and reduce the dynamic effects. The aerodynamic torque can be used to actively compensate the system disturbance in y and z axes of the body system without knowing structural parameters of the satellite. The numerical simulation indicates that the satellite is capable of maintaining the attitude convergence accuracy within ±0.1° all the time despite strong and uncertain aerodynamic torque. The results verify the feasibility and effectiveness of the proposed control scheme for the satellite with moving masses and reaction wheels.**

***Keywords-attitude control; aerodynamic force; moving mass; numerical simulation***

## I. INTRODUCTION

The low Earth orbit (LEO) satellites have very important application value in both civil and military fields[1]. However, the lower the orbit height, the stronger the influence of aerodynamic torque is. Most current attitude control methods are to generate reverse torque to compensate the aerodynamic torque[2]. It leads that the reaction wheel speed will be easily saturated, or too much propellant will be consumed. Therefore, this study investigates a method of using a moving mass actuator to assist the traditional reaction wheel actuator to minimize the aerodynamic torque of the LEO satellite.

In fact, the interaction forces between the body and moving masses are proposed to directly control the attitude. Edwards et al.[3] proposed a method of converting uncontrolled tumbling motion into simple spin by one moving mass. Kumar and Zou[4] proposed to control the attitude directly by utilizing interaction forces from one internal mass. He et al.[5] investigated a novel mass-shifting procedure and a small-angle maneuver method to achieve a full-domain attitude reorientation. However, in these studies, the spacecraft was simplified to be free from external forces, and only the interaction forces. This approach does not apply to the LEO satellite with strong aerodynamic forces.

Thereafter, enlightened by the re-entry control of the warhead with moving masses[6], a novel method of using moving mass actuators to actively control aerodynamic torque was proposed for the LEO satellite. The centre of mass (CoM) is controlled to change the vector from the CoM to the centre of pressure (CoP). In particular, He et al.[7] investigated the feasibility of using four movable masses to realize three-axis attitude stabilization by using internal momentum exchange torque and aerodynamic torque. Lu[8] designed a double symmetric moving mass system for the three-axis stabilization of a 2U LEO CubeSat. To avoid being underactuated, Chesi[9]-[10] first proposed to complement the moving mass system with another traditional actuator. Virgili-Llop et al.[11]-[12] analysed the uncertainties of the aerodynamic model and developed a quaternion feedback control law. Hu et al.[13] designed a dynamic surface attitude control scheme to solve multiple practical problems of the LEO satellite with moving masses. However, these methods essentially belong to the passive attitude control method. A high precision attitude is difficult to achieve, and its attitude control ability is insufficient.

This study extends the application of the moving mass actuator in the attitude control of the LEO satellite. By using the moving mass actuator to assist the reaction wheel actuator, the problem that the aerodynamic torque seriously affects the attitude is solved. The rotational dynamic equations and the translational dynamic equations are derived by Newtonian mechanics, and the mechanism of the dynamic effects of the movement is analysed. In addition, a control method is designed considering the uncertainties of the atmospheric environment and the dynamic effects. Numerical simulation is conducted to verify the feasibility of the proposed control scheme for the satellite with moving masses and reaction wheels.

## II. MODELLING

To obtain higher attitude control accuracy and stronger attitude control ability, this study uses reaction wheels as the active attitude control actuator, and the moving mass actuator is used to solve the problem of the strong

978-1-7281-9768-5/21/$31.00 ©2021 IEEE
DOI 10.1109/ICMEAS54189.2021.00017

aerodynamic disturbance. Notably, most LEO satellites fly with the smallest windward attitude. Considering that aerodynamic force must be in the opposite direction of the satellite flight direction, the moving mass actuator is designed to be able to change the position of the CoM only in the plane perpendicular to aerodynamic force, as shown in figure 1.

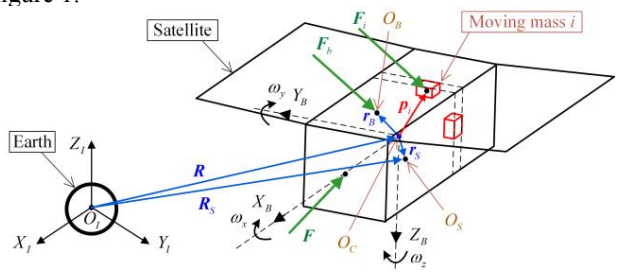


Figure 1. Force diagram of the satellite system.

Symbolic explanation:

1) The systems $O_I X_I Y_I Z_I$ and $O_C X_B Y_B Z_B$ denote the inertia coordinate system and the body coordinate system, respectively. $O_S$ and $O_C$ are the CoM of the system (including the masses) and the centroid of the satellite, respectively. $O_B$ is the CoM of the body (without the masses).

2) The vectors $\boldsymbol{R}$ and $\boldsymbol{R}_S$ locate $O_C$ and $O_S$ in the $O_I X_I Y_I Z_I$ system, respectively. The vectors $\boldsymbol{r}_B$ and $\boldsymbol{r}_S$ locate $O_B$ and $O_S$ in the $O_C X_B Y_B Z_B$ system, respectively. The vector $\boldsymbol{p}_i$ locates the moving mass $i$ in the $O_C X_B Y_B Z_B$ system.

3) $\boldsymbol{F}_b$ is the resultant external force applied to the body. $\boldsymbol{F}_i$ is the resultant force acting on mass $i$. $\boldsymbol{F}$ is the resultant external force applied to the system.

4) The angular velocity vector of the $O_C X_B Y_B Z_B$ system with respect to the $O_I X_I Y_I Z_I$ system expressed in the $O_C X_B Y_B Z_B$ system is defined as $\boldsymbol{\omega}$.

5) The mass of the body and the mass $i$ are $M$ and $m_i$. The inertia matrix of the body is $\boldsymbol{J}_B$.

6) The operation $\hat{\dot{\boldsymbol{x}}}$ is the second derivative with respect to the $O_I X_I Y_I Z_I$ system. The operations $\dot{\boldsymbol{x}}$ and $\ddot{\boldsymbol{x}}$ are the first and second derivatives with respect to the $O_C X_B Y_B Z_B$ system. $[\bullet]^{\times}$ represents the cross-product operator.

### *A. Dynamic Equations of the Satellite with Moving Masses*

Due to the high density and the small size of moving masses, each moving mass is assumed as a point mass. From Newtonian mechanics, the force equations can be stated as

$$\begin{aligned} &\boldsymbol{F}_b = M\left(\hat{\ddot{\boldsymbol{R}}} + \hat{\ddot{\boldsymbol{r}}}_B\right),\ \ \boldsymbol{F}_i = m_i\left(\hat{\ddot{\boldsymbol{R}}} + \hat{\ddot{\boldsymbol{p}}}_i\right), \\ &\boldsymbol{F} = \boldsymbol{G} + \boldsymbol{F}_e = \boldsymbol{F}_b + \sum_{i=1}^{n}\boldsymbol{F}_i = M\left(\hat{\ddot{\boldsymbol{R}}} + \hat{\ddot{\boldsymbol{r}}}_B\right) + \sum_{i=1}^{n} m_i\left(\hat{\ddot{\boldsymbol{R}}} + \hat{\ddot{\boldsymbol{p}}}_i\right) \end{aligned} \tag{1}$$

where, $\boldsymbol{F}_e$ is the environmental force except for the gravity of the system $\boldsymbol{G}$.

From the vector differentiation rule, $\hat{\ddot{\boldsymbol{p}}}_i$ and $\hat{\ddot{\boldsymbol{r}}}_B$ can be stated as

$$\hat{\ddot{\boldsymbol{p}}}_i = \ddot{\boldsymbol{p}}_i + 2\boldsymbol{\omega}\times\dot{\boldsymbol{p}}_i + \dot{\boldsymbol{\omega}}\times\boldsymbol{p}_i + \boldsymbol{\omega}\times\left(\boldsymbol{\omega}\times\boldsymbol{p}_i\right) \tag{2}$$

$$\hat{\ddot{\boldsymbol{r}}}_B = \dot{\boldsymbol{\omega}}\times\boldsymbol{r}_B + \boldsymbol{\omega}\times\left(\boldsymbol{\omega}\times\boldsymbol{r}_B\right) \tag{3}$$

It is noted that $\hat{\ddot{\boldsymbol{R}}}_S$ denotes the absolute acceleration of $O_S$. Thus, the gravity $\boldsymbol{G}$ can be expressed as $\left(M + \sum_{i=1}^{n} m_i\right)\hat{\ddot{\boldsymbol{R}}}_S$. Using Eq. (1) and the fact that $\hat{\ddot{\boldsymbol{r}}}_S = -\hat{\ddot{\boldsymbol{R}}} + \hat{\ddot{\boldsymbol{R}}}_S$, it yields:

$$\hat{\ddot{\boldsymbol{r}}}_S = -\left(\boldsymbol{F}_e - M\hat{\ddot{\boldsymbol{r}}}_B - \sum_{i=1}^{n} m_i\hat{\ddot{\boldsymbol{p}}}_i\right)\Big/\left(M + \sum_{i=1}^{n} m_i\right) \tag{4}$$

The mass $i$ is subjected to the force $\boldsymbol{f}_i$ applied by the body and its gravity. The force $\boldsymbol{f}_i$ can be expressed as

$$\boldsymbol{f}_i = m_i\left(-\hat{\ddot{\boldsymbol{r}}}_S + \hat{\ddot{\boldsymbol{p}}}_i\right) \tag{5}$$

The centroid of the satellite $O_C$ is subjected to the following four torques:

The first one is the torque $\boldsymbol{T}_B = \boldsymbol{r}_B \times M\hat{\ddot{\boldsymbol{r}}}_S$ of the resultant external force applied to the body relative to $O_C$. The second one is the torque $\boldsymbol{T}_m = -\sum_{i=1}^{n}\boldsymbol{p}_i\times\boldsymbol{f}_i$ that the moving masses apply to $O_C$. The third one is the torque of environmental force relative to $O_C$, and it can be expressed as $\boldsymbol{T}_e = \boldsymbol{r}_P \times \boldsymbol{F}_e$ where $\boldsymbol{r}_P$ locates the CoP of the satellite in the $O_C X_B Y_B Z_B$ system. The fourth one is the control torque $\boldsymbol{T}_W$ of reaction wheels.

Thus, the dynamic equation of the attitude is given by

$$\boldsymbol{J}_B\dot{\boldsymbol{\omega}} + \boldsymbol{\omega}\times\left(\boldsymbol{J}_B\boldsymbol{\omega} + \boldsymbol{C}\boldsymbol{I}_W\boldsymbol{\omega}_W\right) = \boldsymbol{T}_B + \boldsymbol{T}_m + \boldsymbol{T}_e + \boldsymbol{T}_W \tag{6}$$

where, $\boldsymbol{C}$ is the installation matrix of the reaction wheel actuator; $\boldsymbol{I}_W$ and $\boldsymbol{\omega}_W$ are the inertia matrix and the angular velocity of reaction wheels; $\boldsymbol{T}_W = \boldsymbol{C}\boldsymbol{I}_W\dot{\boldsymbol{\omega}}_W$.

Substituting from Eq. (5) into $\boldsymbol{T}_m$ and the fact that $\boldsymbol{r}_S = \left(M\boldsymbol{r}_B + \sum_{i=1}^{n} m_i\boldsymbol{p}_i\right)\Big/\left(M + \sum_{i=1}^{n} m_i\right)$, it yields:

$$
\begin{aligned}
&\boldsymbol{T}_e + \boldsymbol{T}_B + \boldsymbol{T}_m \\
&= \boldsymbol{r}_P \times \boldsymbol{F}_e - \boldsymbol{r}_S \times \left( \boldsymbol{F}_e - M\hat{\ddot{\boldsymbol{r}}}_B - \sum_{i=1}^{n} m_i \hat{\ddot{\boldsymbol{p}}}_i \right) - \sum_{i=1}^{n} \left( m_i \boldsymbol{p}_i \times \hat{\ddot{\boldsymbol{p}}}_i \right) \\
&= \left( \boldsymbol{r}_P - \boldsymbol{r}_S \right) \times \boldsymbol{F}_e - \boldsymbol{J}_M \dot{\boldsymbol{\omega}} - \boldsymbol{\omega} \times \boldsymbol{J}_M \boldsymbol{\omega} + \boldsymbol{M}_a + \boldsymbol{M}_c
\end{aligned} \tag{7}
$$

where, $\boldsymbol{J}_M$ is the additional moment of inertia related to $\boldsymbol{p}_i$; $\boldsymbol{M}_a$ is the additional inertial torque related to $\ddot{\boldsymbol{p}}_i$; $\boldsymbol{M}_c$ is the additional Coriolis torque related to $\dot{\boldsymbol{p}}_i$.

Substitution from Eq. (2) and Eq. (3) into Eq. (7) yields

$$
\begin{cases}
\boldsymbol{J}_M = \left( M + \sum_{i=1}^{n} m_i \right) \left[ \boldsymbol{r}_S \right]^{\times} \left[ \boldsymbol{r}_S \right]^{\times} - \sum_{i=1}^{n} m_i \left[ \boldsymbol{p}_i \right]^{\times} \left[ \boldsymbol{p}_i \right]^{\times} \\
\boldsymbol{M}_a = \boldsymbol{r}_S \times \sum_{i=1}^{n} m_i \ddot{\boldsymbol{p}}_i - \sum_{i=1}^{n} \left( m_i \boldsymbol{p}_i \times \ddot{\boldsymbol{p}}_i \right) \\
\boldsymbol{M}_c = 2\boldsymbol{r}_S \times \left( \boldsymbol{\omega} \times \sum_{i=1}^{n} m_i \dot{\boldsymbol{p}}_i \right) - \sum_{i=1}^{n} \left[ 2m_i \boldsymbol{p}_i \times \left( \boldsymbol{\omega} \times \dot{\boldsymbol{p}}_i \right) \right]
\end{cases} \tag{8}
$$

By combining Eq. (6) and Eq. (7), the complete attitude dynamic equation can be written as

$$
\begin{aligned}
&\left( \boldsymbol{J}_B + \boldsymbol{J}_M \right) \dot{\boldsymbol{\omega}} + \boldsymbol{\omega} \times \left[ \left( \boldsymbol{J}_B + \boldsymbol{J}_M \right) \boldsymbol{\omega} + \boldsymbol{C}\boldsymbol{I}_W \boldsymbol{\omega}_W \right] \\
&= \left( \boldsymbol{r}_P - \boldsymbol{r}_S \right) \times \boldsymbol{F}_e + \boldsymbol{M}_a + \boldsymbol{M}_c + \boldsymbol{T}_W
\end{aligned} \tag{9}
$$

It is assumed that there are two moving masses in the satellite, which can respectively move along two straight lines parallel to y and z axes of the $O_C X_B Y_B Z_B$ system. The position vectors of two moving masses are given by $\boldsymbol{p}_1 = \left[ \delta_x \quad l_1 \quad \delta_z \right]$ and $\boldsymbol{p}_2 = \left[ \delta_x \quad \delta_y \quad l_2 \right]$, where, $\delta_x$, $\delta_y$, and $\delta_z$ are installation parameters; $l_1$ and $l_2$ are positions of two masses, respectively.

Defining constant matrices $\boldsymbol{b}_1 = \left[ 0 \quad 1 \quad 0 \right]$ and $\boldsymbol{b}_2 = \left[ 0 \quad 0 \quad 1 \right]$, and combining (5), the translational dynamic equations of the moving masses can be written as

$$
u_i = m_i \boldsymbol{b}_i \left( \frac{\boldsymbol{F}_e - M\hat{\ddot{\boldsymbol{r}}}_B - m_1 \hat{\ddot{\boldsymbol{p}}}_1 - m_2 \hat{\ddot{\boldsymbol{p}}}_2}{M + m_1 + m_2} + \hat{\ddot{\boldsymbol{p}}}_i \right) \tag{10}
$$

where, $u_i$ is the driving force of each moving mass.

### *B. Attitude Kinematics and Dynamics Relative to the Orbit System*

The orbit coordinate system $O_O X_O Y_O Z_O$ is here defined. The angular velocity of the satellite in the $O_O X_O Y_O Z_O$ system is $\boldsymbol{\omega}_{bo} = \boldsymbol{\omega} - \boldsymbol{A}_{bo} \boldsymbol{\omega}_{oi}$, where $\boldsymbol{A}_{bo}$ denotes the direction cosine matrix from the $O_O X_O Y_O Z_O$ system to the $O_C X_B Y_B Z_B$ system, and $\boldsymbol{\omega}_{oi}$ represents the orbital angular velocity expressed in the $O_O X_O Y_O Z_O$ system.

Considering the fact that $\dot{\boldsymbol{A}}_{bo} = -\boldsymbol{\omega}_{bo} \times \boldsymbol{A}_{bo}$ and $\dot{\boldsymbol{\omega}}_{oi} = 0$, the time derivative of the angular velocity is $\dot{\boldsymbol{\omega}}_{bo} = \dot{\boldsymbol{\omega}} + \boldsymbol{\omega}_{bo} \times \boldsymbol{A}_{bo} \boldsymbol{\omega}_{oi}$. Thus, the attitude dynamic equation relative to the $O_O X_O Y_O Z_O$ system is

$$
\begin{aligned}
\dot{\boldsymbol{\omega}}_{bo} &= \boldsymbol{\omega}_{bo} \times \boldsymbol{A}_{bo} \boldsymbol{\omega}_{oi} \\
&+ \left( \boldsymbol{J}_B + \boldsymbol{J}_M \right)^{-1} \left( -\boldsymbol{\omega} \times \left[ \left( \boldsymbol{J}_B + \boldsymbol{J}_M \right) \boldsymbol{\omega} + \boldsymbol{C}\boldsymbol{I}_W \boldsymbol{\omega}_W \right] \right) \\
&+ \left( \boldsymbol{J}_B + \boldsymbol{J}_M \right)^{-1} \left[ \left( \boldsymbol{r}_P - \boldsymbol{r}_S \right) \times \boldsymbol{F}_e + \boldsymbol{M}_a + \boldsymbol{M}_c + \boldsymbol{T}_W \right]
\end{aligned} \tag{11}
$$

In this study, the modified Rodrigues parameter (MRS) $\boldsymbol{\sigma}_{bo}$ is used to represent the attitude mapping from the $O_O X_O Y_O Z_O$ system to the $O_C X_B Y_B Z_B$ system. The attitude kinematic equation relative to the $O_O X_O Y_O Z_O$ system based on MRS is

$$
\dot{\boldsymbol{\sigma}}_{bo} = \boldsymbol{G}\left( \boldsymbol{\sigma}_{bo} \right) \boldsymbol{\omega}_{bo} \tag{12}
$$

where, $\boldsymbol{G}\left( \boldsymbol{\sigma}_{bo} \right) = \frac{1}{2} \left( \boldsymbol{I}_{3\times3} + \left[ \boldsymbol{\sigma}_{bo} \right]^{\times} + \boldsymbol{\sigma}_{bo} \boldsymbol{\sigma}_{bo}^{\ T} - \frac{1 + \boldsymbol{\sigma}_{bo}^{\ T} \boldsymbol{\sigma}_{bo}}{2} \boldsymbol{I}_{3\times3} \right)$; $\boldsymbol{I}_{3\times3} \in \boldsymbol{R}^{3\times3}$ denotes the identity matrix.

## III. CONTROLLER DESIGN

The aerodynamic disturbance that always exists would lead to frequent saturation of the reaction wheel speed[14]. Therefore, a moving mass actuator is used to adjust the vector from $O_S$ to the CoP of the satellite as parallel as possible to the aerodynamic force, so as to minimize the influence of the aerodynamic torque. Considering that the CoM of system can only be moved in the $O_C X_B Y_B$ plane in this study, the moving mass actuator will not execute the control command until the attitude is three-axis stable, as shown in figure 2. The estimated value of the aerodynamic torque is substituted into the control algorithm.

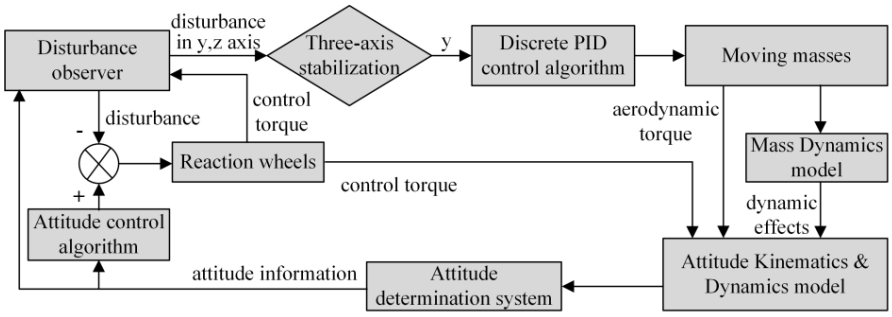


Figure 2. The flow diagram of the control system.

*A. Nonlinear Disturbance Observer Design*

The system disturbance is defined as $\boldsymbol{d}=(\boldsymbol{r}_P-\boldsymbol{r}_S)\times\boldsymbol{F}_e+\boldsymbol{M}_a+\boldsymbol{M}_c$, and its estimated value is defined as $\hat{\boldsymbol{d}}$. The time derivative of $\hat{\boldsymbol{d}}$ is defined as $\dot{\hat{\boldsymbol{d}}}=K(\boldsymbol{d}-\hat{\boldsymbol{d}})$, where $K>0$ is the gain of the observer.

An auxiliary variable vector $\boldsymbol{z}$ is defined as $\boldsymbol{z}=\hat{\boldsymbol{d}}-K(\boldsymbol{J}_B+\boldsymbol{J}_M)\boldsymbol{\omega}_{bo}$ [15]. Combining Eq. (11) and taking the time derivative of $\boldsymbol{z}$, the nonlinear observer is given by

$$\begin{cases}\dot{\boldsymbol{z}}=K\left(\boldsymbol{\omega}\times\left[(\boldsymbol{J}_B+\boldsymbol{J}_M)\boldsymbol{\omega}+\boldsymbol{C}\boldsymbol{I}_W\boldsymbol{\omega}_W\right]\right)\\ \quad -K(\boldsymbol{J}_B+\boldsymbol{J}_M)(\boldsymbol{\omega}_{bo}\times\boldsymbol{A}_{bo}\boldsymbol{\omega}_{oi})-K\boldsymbol{T}_W-K\hat{\boldsymbol{d}}\\ \hat{\boldsymbol{d}}=\boldsymbol{z}+K(\boldsymbol{J}_B+\boldsymbol{J}_M)\boldsymbol{\omega}_{bo}\end{cases}\tag{13}$$

Since, the disturbance $\boldsymbol{d}$ varies slowly relative to the observer dynamics in this study, it is reasonable to suppose that $\dot{\boldsymbol{d}}=0$. The observer error is defined as $\tilde{\boldsymbol{d}}=\boldsymbol{d}-\hat{\boldsymbol{d}}$. The observer error equation is $\dot{\tilde{\boldsymbol{d}}}+K\tilde{\boldsymbol{d}}=0$, and its analytical solution is $\tilde{\boldsymbol{d}}(t)=\tilde{\boldsymbol{d}}(t_0)e^{-Kt}$.

Thus, the observer is globally asymptotically stable and $\tilde{\boldsymbol{d}}$ converges to zero at the exponential rate. In view of the effective compensation, the controller can provide a fast and accurate response.

*B. Attitude Control Algorithm Design*

In this study, the attitude control target is three-axis stabilization, that is, $\boldsymbol{\sigma}_{bo}\to 0$ and $\boldsymbol{\omega}_{bo}\to 0$. The sliding mode function is designed as $\boldsymbol{s}=\boldsymbol{c}\boldsymbol{\sigma}_{bo}+\boldsymbol{\omega}_{bo}$, where, $\boldsymbol{c}=\mathrm{diag}(c_1\quad c_2\quad c_3)$ and $c_1,c_2,c_3>0$.

$$\begin{aligned}\boldsymbol{T}_W=(\boldsymbol{J}_B+\boldsymbol{J}_M)\left[-\boldsymbol{c}\boldsymbol{G}(\boldsymbol{\sigma}_{bo})\boldsymbol{\omega}_{bo}-\boldsymbol{\omega}_{bo}\times\boldsymbol{A}_{bo}\boldsymbol{\omega}_{oi}-\boldsymbol{k}\boldsymbol{s}\right]\\ +\boldsymbol{\omega}\times\left[(\boldsymbol{J}_B+\boldsymbol{J}_M)\boldsymbol{\omega}+\boldsymbol{C}\boldsymbol{I}_W\boldsymbol{\omega}_W\right]-\hat{\boldsymbol{d}}\end{aligned}\tag{14}$$

where, $\boldsymbol{k}=\mathrm{diag}(k_1\quad k_2\quad k_3)$ and $k_1,k_2,k_3>0$.

To prove the convergence of the attitude, a Lyapunov function is designed as $V=\left(\boldsymbol{s}^T\boldsymbol{s}+\tilde{\boldsymbol{d}}^T\tilde{\boldsymbol{d}}\right)/2$. Combining Eq. (14) and taking the time derivative of the Lyapunov function and, it yields:

$$\begin{aligned}\dot{V}&=\boldsymbol{s}^T\dot{\boldsymbol{s}}+\tilde{\boldsymbol{d}}^T\dot{\tilde{\boldsymbol{d}}}\\ &=\boldsymbol{s}^T\left[-\boldsymbol{k}\boldsymbol{s}-(\boldsymbol{J}_B+\boldsymbol{J}_M)^{-1}\tilde{\boldsymbol{d}}\right]-K\left\|\tilde{\boldsymbol{d}}\right\|^2\le 0\end{aligned}\tag{15}$$

Notably, the inequality in Eq. (15) is correct as the observed value $\hat{\boldsymbol{d}}$ can precisely track the disturbance $\boldsymbol{d}$ [16], which is proved in subsection 3.1. Thus, it can be concluded that, by choosing the proper parameters $K$, $\boldsymbol{c}$, and $\boldsymbol{k}$, the attitude error can be adjusted to be arbitrarily small.

*C. Mass Movement Control Algorithm Design*

To simplify the control scheme, the input signal of the moving mass actuator is the position of each mass $l_i$ rather than the driving force $u_i$. In fact, this simplification is reasonable since most linear motors are servo-actuated. In addition, the dynamic effects of the movement of masses are considered as a part of system disturbance, and it can be significantly reduced by slowing down the movement of masses, seen from Eq. (8). Therefore, an incremental discrete PID algorithm [17] is designed to control the position of each mass.

After the attitude is three-axis stable, the target of mass movement control algorithm is to minimize the system disturbance in $O_CY_B$ and $O_CZ_B$ axes, that is, $\hat{d}_2\to 0$ and $\hat{d}_3\to 0$. Thus, the incremental discrete PID control laws are given by

$$\begin{aligned}\Delta l_1&=k_p\left[\hat{d}_3(kT)-\hat{d}_3\left((k-1)T\right)\right]+k_i\hat{d}_3(kT)\\ &+k_d\left[\hat{d}_3(kT)-2\hat{d}_3\left((k-1)T\right)+\hat{d}_3\left((k-2)T\right)\right]\end{aligned}\tag{16}$$

$$\begin{aligned}\Delta l_2&=k_p\left[\hat{d}_2(kT)-\hat{d}_2\left((k-1)T\right)\right]+k_i\hat{d}_2(kT)\\ &+k_d\left[\hat{d}_2(kT)-2\hat{d}_2\left((k-1)T\right)+\hat{d}_2\left((k-2)T\right)\right]\end{aligned}\tag{17}$$

where, $\Delta l_1$ and $\Delta l_2$ are the increment of positions; $k_p$, $k_i$, and $k_d$ are the control parameters; $T$ is the period of the discrete control.

It is noted that, as long as the estimation is accurate, even if there are uncertainties in the aerodynamic environment, the aerodynamic torque can still be minimized.

## IV. SIMULATION

In this study, a numerical simulation platform is developed in the Matlab/Simulink environment. The developed control scheme is applied to a LEO small satellite, as shown in figure 1. The given stroke limitation of each mass is ±200 mm; thus, the adjustable range of the CoM in the $O_C Y_B$ and $O_C Z_B$ axes is ±20 mm. The parameters of the satellite and the control law are listed in table 1.

TABLE I. PARAMETERS OF THE SATELLITE AND CONTROLLER

| Parameters | Value |
|---|---|
| Mass | $M = 80$ kg, $m_1 = m_2 = 10$ kg |
| Moment of inertia | $\boldsymbol{J}_B = \mathrm{diag}(5,15,12)$ kg·m$^2$, $\boldsymbol{I}_W = \mathrm{diag}(0.05,0.1,0.1)$ kg·m$^2$ |
| Installation parameters | $\delta_x = \delta_y = \delta_z = 0$, $\boldsymbol{C} = \boldsymbol{I}_{3\times3}$ |
| Satellite parameters | $\boldsymbol{r}_P = [-0.01,0,0.01]$ m, $\boldsymbol{r}_B = [0.01,0.02,-0.01]$ m |
| Initial attitude | $\boldsymbol{\sigma}_{bo0} = [0.04;0.04;-0.05]$, $\boldsymbol{\omega}_{bo0} = [0;0;0]$ rad/s |
| Orbital angular velocity | $\boldsymbol{\omega}_{oi} = [0;-0.0015;0]$ rad/s |
| Aerodynamic force | $\boldsymbol{F}_e = \left(1+0.3\cos\frac{\pi}{2700}t\right)\boldsymbol{A}_{bo}[-0.02;0;0]$ N |
| Parameters of controller | $K = 1$, $\boldsymbol{c} = \mathrm{diag}(0.04,0.05,0.05)$, $\boldsymbol{k} = \mathrm{diag}(0.015,0.02,0.02)$, $k_p = k_i = k_d = 50$ |

In this simulation, the dynamic update period is 100 ms, and the total simulation time is 3000 s. The disturbance observer is updated according to the measurement frequency, which is 2 Hz in this simulation. The update period of the attitude control algorithm is 1 s. In addition, the update period of the mass movement control algorithm is 50 s, and, in each control period, every moving mass moves to its target position in a sinusoidal curve. The simulation results are presented in figures 3-5:

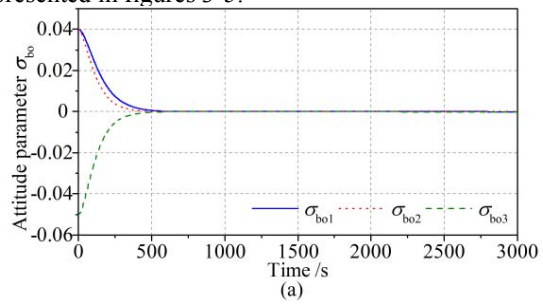


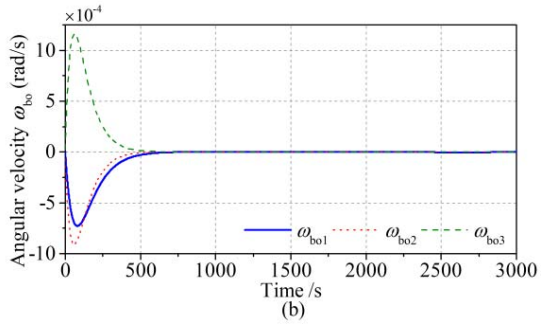


Figure 3. Curves of the attitude parameters.

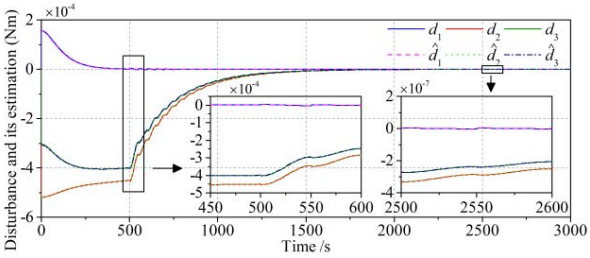


Figure 4. Tracking curves of the system disturbance.

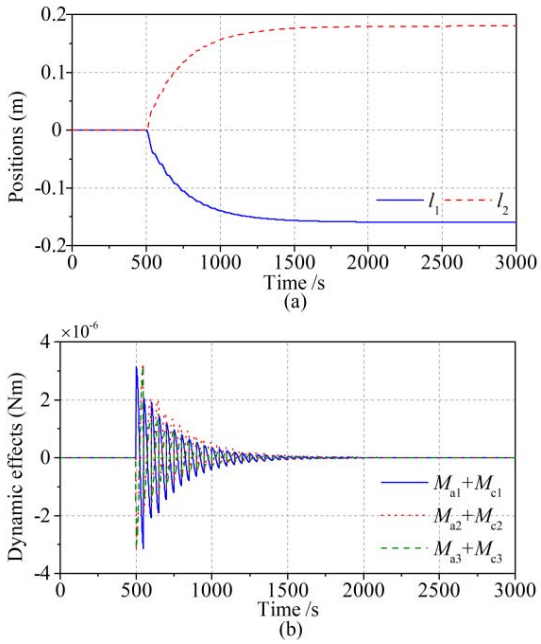


Figure 5. Curves of positions of masses and corresponding dynamic effects.

As shown in figure 3, the attitude of the satellite is three-axis stable in about 500 s, and then it can maintain a convergence accuracy of ±0.1° all the time. It proves that the proposed control scheme of using a moving mass actuator to assist the reaction wheel actuator is very suitable for the LEO satellite with the strong aerodynamic disturbance, and a high precision attitude can be achieved.

Figure 4 shows the time response of the nonlinear disturbance observer. It can be seen that the nonlinear

observer can achieve the precise estimation of the system disturbance. Using this estimated value as the feedforward input of attitude control algorithm can effectively improve the accuracy of attitude control. After three-axis stabilization of the attitude, the moving mass actuator starts to execute the control command, and, as expected, the system disturbance in $O_C Y_B$ and $O_C Z_B$ axes would gradually decrease to zero. It proves that this control scheme can minimize the aerodynamic disturbance despite the existence of the uncertainties of the atmospheric environment. Moreover, even if there are some other unknown disturbances in $O_C Y_B$ and $O_C Z_B$ axes, this control scheme can still control the aerodynamic torque to actively compensate them. Notably, due to the use of the discrete control algorithm, the mass movement is significantly slowed down, and its dynamic effects can be ignored compared to other disturbances.

As shown in figure 5, even if $\boldsymbol{r}_B$ and $\boldsymbol{r}_P$ are unknown, the vector from $O_S$ to $O_P$ can still be controlled to be parallel to the aerodynamic force by the feedback control law, so as to decrease the aerodynamic disturbance in $O_C Y_B$ and $O_C Z_B$ axes to zero. However, if the distance between $O_S$ and $O_P$ is too large, the masses will only be controlled to its limiting position, and thus, the system disturbance in $O_C Y_B$ and $O_C Z_B$ axes will not decrease to zero, but its minimum value. In addition, after the aerodynamic disturbance is minimized, the positions of masses tend to be constant, and the dynamic effects decrease to zero. It is helpful to improve the stability of satellite attitude control.

## V. CONCLUSIONS

In this study, a novel attitude control method of using a moving mass actuator to assist the traditional reaction wheel actuator is proposed to deal with the problem of strong aerodynamic torque in LEO. The attitude dynamic equations of the LEO satellite and the translational dynamic equations of the moving masses are derived. By analysing the dynamics, it is found that the dynamic effects of mass movement are related to the velocity and acceleration of masses. A control scheme is designed including nonlinear disturbance observer, sliding mode algorithm for attitude control, and incremental discrete PID algorithm for mass movement. The results of the numerical simulation revealed that the LEO satellite can maintain a high precision attitude for a long time based on the moving mass actuator and the reaction wheel actuator. After the moving mass actuator starts to execute the control command, the system disturbance in $O_C Y_B$ and $O_C Z_B$ axes can be compensated by the aerodynamic torque, so as to decrease to zero. Due to the use of the discrete control algorithm, the dynamic effects of mass movement can be reduced to be negligible. Thus, the feasibility and effectiveness of the proposed control scheme is verified. However, the control scheme in this study is designed only for the three-axis stabilized LEO satellite. In the future, more works will be done on the practical applications of the moving mass actuator.


## ACKNOWLEDGMENT

R.B.G. thanks the support of the National Natural Science Foundation of China under Grant 61803204 and the Natural Science Foundation of Jiangsu Province under Grant BK20180465.


## REFERENCES


[1] A. Shahrooei and M. H. Kazemi, "Multiple model adaptive attitude control of LEO satellite with angular velocity constraints," Int. J. Aeronaut. Space, vol. 19, Mar. 2018, pp. 153–163, doi: 10.1007/s42405-018-0013-7.

[2] X. H. Zhang, X. Zhang, Z. L. Lu and W. H. Liao, "Optimal path planning-based finite-time control for agile CubeSat attitude maneuver," IEEE ACCESS, vol. 7, 2019, pp. 102186–98, doi: 10.1109/ACCESS.2019.2927401.

[3] T. L. Edwards and M. H. Kaplan, "Automatic spacecraft detumbling by internal mass motion," AIAA J., vol. 12, Apr. 1974, pp. 496–502, doi: 10.2514/3.49275.

[4] K. D. Kumar and A. M. Zhou, "Attitude control of miniature satellites using movable masses," SpaceOps 2010 Conf. Alabama, pp. 1–6, April 2010.

[5] L. He, T. Sheng, K. D. Kumar, Y. Zhao, D. Ran and X. Q. Chen, "Attitude maneuver of a satellite using movable masses," Acta Astronaut., vol. 176, Nov. 2020, pp. 464–475, doi: 10.1016/j.actaastro.2020.06.019.

[6] J. E. White and R. D. Robinett, "Principal axis misalignment control for deconing of spinning spacecraft," J. Guid. Control Dynam., vol. 17, No. 4, Jul. 1994, pp. 823–830, doi: 10.2514/3.21272.

[7] L. He, X. Q. Chen, K. D. Kumar, T. Sheng and C. F. Yue, "A novel three-axis attitude stabilization method using in-plane internal mass-shifting," Aerosp. Sci. Technol., vol. 92, Sept. 2019, pp. 489–500, doi: 10.1016/j.ast.2019.06.019.

[8] Z. L. Lu, "Study on mass moment attitude control for fast orbit maneuver satellite," PhD Thesis, Nanjing: Nanjing University of Science and Technology, 2017.

[9] S. Chesi, "Attitude control of nanosatellites using shifting masses," PhD Thesis, California: University of California, 2015.

[10] S. Chesi, Q. Gong and M. Romano, "Aerodynamic three-axis attitude stabilization of a spacecraft by center-of-mass shifting," J. Guid. Control Dynam., vol. 40, Jul. 2017, pp. 1613–26, doi: 10.2514/1.G002460.

[11] J. Virgili-Llop, H. C. Polat and M. Romano, "Using shifting masses to reject aerodynamic perturbations and to maintain a stable attitude in very low Earth orbit," 26th AAS/AIAA Space Flight Mechanics Meeting Napa CA, Feb. 2016, pp 1–20.

[12] J. Virgili-Llop, H. C. Polat and M. Romano, "Attitude stabilization of spacecraft in very low Earth orbit by center-of-mass shifting," Front. Robot. AI, vol. 6, 2019, pp. 1–19, doi: 10.3389/frobt.2019.00007.

[13] Y. D. Hu, Z. L. Lu and W. H. Liao, "Speed-adaptive dynamic surface attitude control for a satellite with moving masses under input constraints," T. I. Meas. Control, vol. 42, No.16, Dec. 2020, pp. 3091–3109, doi: 10.1177/0142331220940427.

[14] A. M. Zou, H. J. Ruiter and K. D. Kumar, "Finite-time attitude tracking control for rigid spacecraft with control input constraints," IET Control Theory A., vol. 11, Apr. 2017, pp. 931–940, doi: 10.1049/iet-cta.2016.1097.

[15] W. H. Chen, D. J. Ballance, P. J. Gawthrop and J. O'Reilly, "A nonlinear disturbance observer for robotic manipulators," IEEE T. Ind. Electron., vol. 47, No. 4, Aug. 2000, pp. 932–938, doi: 10.1109/41.857974.

[16] C. J. Zhou, J. H. Zhu, H. M. Lei and X. M. Yuan, "Observer-based dynamic surface control for high-performance aircraft subjected to unsteady aerodynamics and actuator saturation," P. I. Mech. Eng. I-J. Sys., vol. 231, Jul. 2017, pp. 481–494, doi: 10.1177/0959651816689739.

[17] H. S. Khan and M. B. Kadri, “Attitude and altitude control of quadrotor by discrete PID control and non-linear model predictive control,” 2015 Int. Conf. on Information and Communication Technologies, Dec. 2015, pp 1–11, doi: 10.1109/ICICT.2015.7469486.